

Tetrahedra, Super-Tetrahedra, Bipyramids, Boxes and More: Polymetallic Clusters of Benzotriazole

David Collison,^[a] Eric J. L. McInnes,^{*[a]} and Euan K. Brechin^{*[b]}

Keywords: Benzotriazole / Clusters / Transition metals / Large spin ground states / Single-molecule magnets

The syntheses, structures and magnetic properties of a host of polymetallic 3d transition-metal clusters made with the pro-ligand benzotriazole (BtaH) and its analogues are reported. These range from a family of tetradecametallic clusters with spin ground states as large as $S \approx 25$, to decametal-

lic vanadium "boxes", to iron and manganese tetra- and super-tetrahedra, to hexaicosametallic manganese single-molecule magnets.

(© Wiley-VCH Verlag GmbH & Co. KGaA, 69451 Weinheim, Germany, 2006)

Introduction

The synthesis and characterization of polynuclear clusters of paramagnetic metal ions has attracted intense study

since the discovery that such molecules can display the phenomenon of single-molecule magnetism.^[1] In these molecules there exists an energy barrier to the relaxation of the magnetization due to the combination of a large ground-state spin multiplicity and significant negative magnetoanisotropy. This imparts a molecular magnetic memory effect that can be observed as temperature- and sweep-rate-dependent hysteresis loops in M vs. H studies.^[2]

Single-Molecule Magnets (SMMs) have many potential applications including high-density information storage in

[a] School of Chemistry, The University of Manchester, Oxford Road, Manchester, M13 9PL, UK
E-mail: eric.mcinnnes@manchester.ac.uk

[b] School of Chemistry, The University of Edinburgh, West Mains Road, Edinburgh, EH9 3JJ, UK
E-mail: ebrechin@staffmail.ed.ac.uk



David Collison graduated (University of Manchester) in 1976 and after a PhD (Manchester, with C. D. Garner and I. H. Hillier), and post-doctoral work (Manchester, F E. Mabbs; Manchester, C. D. Garner; UMIST, N. J. Blackburn), became a SRC Fellow (Manchester) and subsequently a Royal Society University Research Fellow (Manchester). He was appointed Senior Lecturer at the University of Manchester in 1994 and promoted to his current position of Reader in 1998. His research concentrates on the electronic structure of transition metals in chemical, biological and materials sciences.



Eric McInnes is a Reader in the School of Chemistry at The University of Manchester. He completed his PhD in 1995 under the supervision of Dr Lesley J. Yellowlees at the University of Edinburgh, where he also obtained his BSc in 1992. He was a post-doctoral researcher in Manchester with Drs. Frank E. Mabbs and David Collison, then at the University of East Anglia with Profs Andrew J. Thomson FRS and Annie K. Powell, before taking a lectureship in Manchester in 2000.



Euan Brechin was born in Greenock, Scotland, in 1972. He completed both his BSc (1994) and PhD (1997) degrees at The University of Edinburgh (UK), the latter under the supervision of Dr R. E. P. Winpenny. After postdoctoral work with Professor George Christou at Indiana University (USA) he was awarded a Lloyd's of London Tercentenary Foundation Fellowship at the University of Manchester (UK). In 2003 he was awarded an EPSRC Advanced Fellowship at the same institution, before moving to his present position at The University of Edinburgh in September 2004.

which each bit of information is stored as the magnetization orientation of an individual molecule, and as qubits for quantum computation where the required arbitrary superposition of quantum states with opposite projections of spin are produced by either quantum tunneling of the magnetization (QTM), intermolecular exchange, or multi-frequency EPR pulses.^[3]

Single-molecule magnetism spans areas as diverse as physics, theoretical chemistry, spectroscopy, materials chemistry and synthetic coordination chemistry, as demonstrated by the several hundred papers published on the topic over the last ten years. There are now several species displaying such behavior – formed by a multitude of successful synthetic strategies ranging from the self-assembly of 3d-metal carboxylate clusters, to molecular Prussian Blues, to heterometallic 3d–4f complexes and most recently to simple 4f monometallic species.^[4] By far the most productive route has been by the self-assembly of 3d transition metals with flexible organic bridging ligands such as carboxylates and alkoxides. Here we describe some of our efforts toward the synthesis of large polymetallic 3d clusters using the ligand benzotriazole (and its analogues), including some of the largest nuclearity and highest-spin ground-state molecules known.

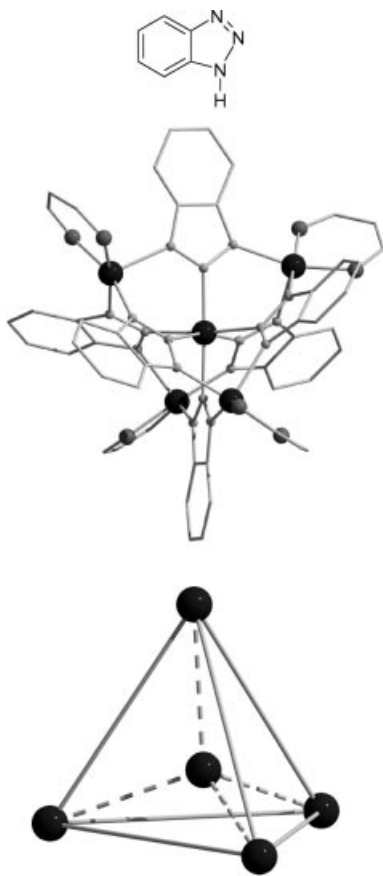


Figure 1. The structure of benzotriazole (BtaH, top); the structure of the complex [Cu₅(Bta)₆(acac)₄] (middle); and its centered tetrahedral {Cu₅} core (bottom). The –CH₃ groups of the acac[−] ligands have been removed for clarity.

Benzotriazole (BtaH, C₆H₅N₃; Figure 1) and substituted benzotriazoles are well established corrosion inhibitors for copper and its alloys,^[5] and as a result the coordination chemistry of benzotriazoles with various M²⁺ species has been thoroughly investigated, producing many new cluster compounds. Of these the most well-known and thoroughly studied are the family of compounds of general formula [M₅(OH)_x(R)_{6−x}(L)₄(H₂O)_{4x}] [where M = Cu, Zn, Ni; R = Bta[−], Me₂Bta[−] (5,6-Me₂-bta[−]); L = β-diketonate, x = 0, 1].^[6] These pentametallic species consist of a tetrahedral arrangement of four M²⁺ ions centered on a fifth, with each μ₃-benzotriazole spanning an edge of the tetrahedron (Figure 1). Magnetic studies have shown that weak antiferromagnetic exchange between the metals leads to spin ground states equal to that of the “isolated” central M²⁺ ion.

Although a number of other Ni²⁺,^[7] Cu²⁺,^[8] Hg²⁺,^[9] Re⁵⁺,^[10] and Ag⁺^[11] complexes have been reported, the chemistry of BtaH and its derivatives with M³⁺ species has, until now, not been investigated.

Our Work

Despite the large numbers of M²⁺ pentamers structurally characterized, only one “related” M³⁺ pentamer has been reported.^[12] The complex [HNEt₃]_x[Fe₅O₂(OMe)₂(Bta)₄-(BtaH)_{1−x}(MeOH)_{5−x}Cl_{5+x}] (1, x = 1, 0; Figure 2) consists of an elongated tetrahedral array of four Fe³⁺ ions centered on a fifth. The central Fe ion is attached to the apical Fe ions by two μ₃-O^{2−} ions forming a [Fe₅O₂]¹¹⁺ core, with the two OMe[−] ligands bridging between the apical Fe ions on each short edge of the elongated tetrahedron and the Bta[−] ligands bridging in a η¹:η¹:μ₂-fashion between the central Fe ion and the apical Fe ions along the long edges of the elongated tetrahedron. The coordination geometry of the apical Fe ions is completed by a combination of terminal Cl[−] and MeOH ligands. The central Fe is antiferromagnetically coupled to the peripheral Fe ions resulting in an S = 15/2 spin ground state (Figure 2), with the best fit obtained for the two independent exchange interactions being J₁ = −7.3 cm^{−1}, J₂ = 8.6 cm^{−1}.^[12] As expected, this suggests that the interaction between the central Fe ion and the apical Fe ions by the μ₃-O^{2−} ions is antiferromagnetic and the interaction between the two apical Fe centers mediated by the μ₂-MeO[−] is ferromagnetic. A spin ground state of S = 15/2 can thus be rationalized by assuming the central Fe is “spin-up” and the apical Fe ions are “spin-down” (Figure 2).

The only other iron cluster containing benzotriazole is the tetradecametallic complex [Fe₁₄O₆(OMe)₁₈(Bta)₆Cl₆] (2, Figure 3) – formed from the reaction between [Fe₃O(OAc)₆(H₂O)₃]Cl and BtaH in MeOH at 100 °C in a Teflon-lined autoclave.^[13] The structure comprises a hexa-capped hexagonal bipyramid of Fe³⁺ ions with caps on alternate faces (Figure 4). The Bta[−] ligands coordinate in the maximal μ₃-mode to form two {Fe₄(Bta)₃} moieties which sandwich a central {Fe₆} ring, bridged by eighteen μ₂-OMe[−] and six μ₄-O^{2−} ions. The {Fe₄(Bta)₃} fragment is reminiscent of the

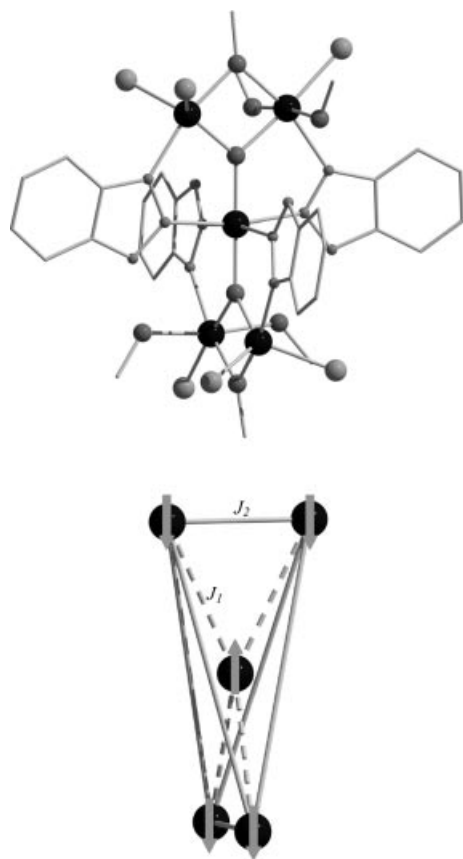


Figure 2. The molecular structure of complex **1** and its elongated, centered tetrahedral $\{\text{Fe}_5\}$ core showing the two independent exchange interactions and the resultant spin topology.

M^{2+} pentamers above (Figure 1) and here they act to stop the growth of the Fe–oxide–alkoxide cluster. Complex **2** exhibits one of the largest spin ground states yet seen with magnetization data suggesting $S \approx 25$ and $D \approx 0 \text{ cm}^{-1}$ (Figure 5).^[13–15] An $S = 25$ ground state can be rationalized from competing antiferromagnetic exchange interactions within the cluster: the relative magnitude of the four chemically distinct, nearest-neighbor exchange pathways via $\mu_4\text{-O}^{2-}$ ions and/or $\mu^2\text{-OMe}^-$ ions can be predicted on the basis of the Fe–O–Fe angles (Figure 4). The Fe(apex)–Fe(face cap) [J_1] and Fe(apex)–Fe(ring) [J_3] interactions are expected to be the most antiferromagnetic because they are defined by the largest angles and therefore dominate over the much weaker antiferromagnetic Fe(face-cap)–Fe(ring) [J_2] and Fe(ring)–Fe(ring) [J_4] interactions. This would lead to a very simple spin structure in the ground state with the two apical Fe ions of the bipyramid “spin down” and all other Fe ions “spin up”. Conventional fitting of the experimental magnetic susceptibility data to a spin Hamiltonian to derive J_1 – J_4 is not possible, but DFT calculations in tandem with Monte Carlo simulations support this model giving: $J_1 = -22 \text{ cm}^{-1}$, $J_2 = -8.7 \text{ cm}^{-1}$, $J_3 = -29.7 \text{ cm}^{-1}$ and $J_4 = -3.7 \text{ cm}^{-1}$.^[14]

Despite its huge ground state S , **2** does not behave as an SMM. This is due to the near isotropic nature of this ground state ($D \approx 0$). However, this is interesting in itself

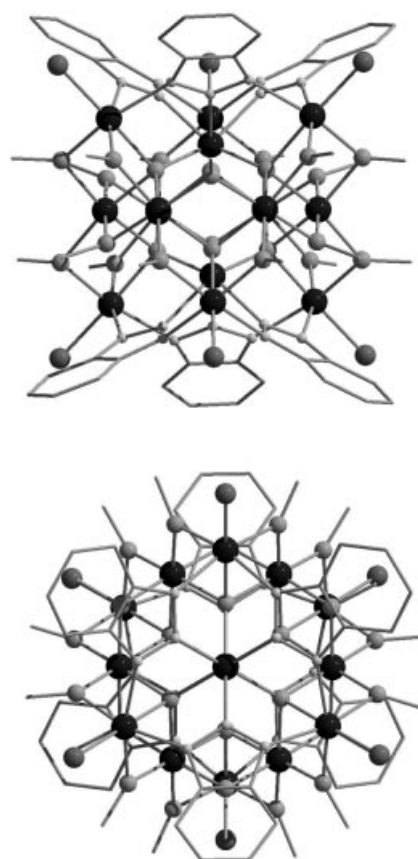


Figure 3. Molecular structure of $[\text{Fe}_{14}\text{O}_6(\text{OMe})_{18}(\text{Bta})_6\text{Cl}_6]$ (**2**) viewed perpendicular (top) and parallel (bottom) to the apical Fe ions.

as it gives rise to an unusually large magnetocaloric effect (MCE) below 10 K.^[15] The 51-fold degeneracy of the (isotropic) ground state gives rise to very large magnetic entropy changes ΔS_m on magnetization. If isothermal magnetization (at temperature T_i) is followed by adiabatic demagnetization then magnetic cooling can be achieved with a characteristic temperature change ΔT_{ad} . The huge spin of **2** (combined with an additional entropy contribution from low-lying excited states) gives rise to $\Delta S_m(T)$ and $\Delta T_{\text{ad}}(T)$ values ($\Delta T_{\text{ad}} = 5.8 \text{ K}$ for $T_i = 6 \text{ K}$) that are not only much larger than those displayed by other molecular clusters but more than 30% larger than any other material for $T_i < 10 \text{ K}$, including the best intermetallic materials such as $[(\text{Dy}_x\text{Er}_{1-x})\text{Al}_2]$.^[16] Thus **2** has potential applications in low temperature magnetic refrigeration.

The analogous clusters $[\text{Cr}_{14}\text{O}_6(\text{OMe})_{18}(\text{Bta})_6\text{Cl}_6]$ (**3**) and $[\text{V}_{14}\text{O}_6(\text{OMe})_{18}(\text{Bta})_6\text{Cl}_6]$ (**4**) can be made in an identical manner,^[17] but in both cases magnetic measurements indicate the complexes to have $S = 0$ spin ground states. This (presumably) arises because of small changes in the relative magnitudes of the four exchange interactions such that the order $|J_3| > |J_1| > |J_2| > |J_4|$ seen in $[\text{Fe}_{14}]$ is not maintained in either $[\text{Cr}_{14}]$ or $[\text{V}_{14}]$.^[17] If the reaction mixture leading to **4** is exposed to atmospheric O_2 then $[(\text{V}^{\text{IV}}\text{O})_6\text{V}^{\text{III}}_8\text{O}_6(\text{OMe})_{18}(\text{Bta})_6]$ (**5**) can be isolated, in which each face cap is oxidized from a $[\text{V}^{\text{III}}\text{-Cl}]^{2+}$ moiety to the isoelectronic

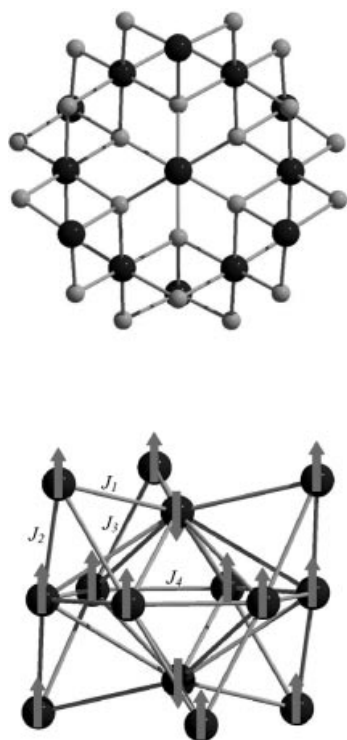


Figure 4. The metal–oxygen core of **2** viewed parallel to the apical Fe ions (top); the hexacapped hexagonal bipyramidal metallic skeleton of **2** (bottom) showing the four independent exchange interactions and the resultant spin topology.

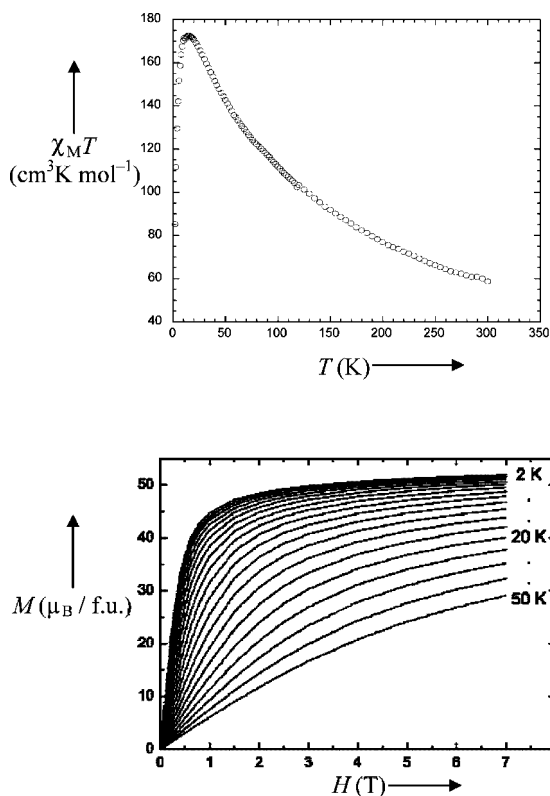


Figure 5. Plot of $\chi_M T$ vs. T for complex **2** in the 300–1.8 K temperature range, and isothermal $M(H)$ curves measured in the temperature range 2–50 K.

vanadyl $[\text{V}^{\text{IV}}=\text{O}]^{2+}$ unit. If these reactions are performed under non-solvothermal, lower temperature conditions then the “box-like” complex $[\text{V}^{\text{IV}}_8\text{V}^{\text{III}}_2\text{O}_8(\text{OH})_4(\text{OMe})_{10}(\text{Bta})_8]$ (**6**) forms (Figure 6).^[18] The complex consists of a square-prism of vanadyl ions where the square faces are bridged through the 1,3-bridging mode of the Bta^- . The “box” surrounds two V^{III} ions that form a $[\text{V}^{\text{III}}_2(\text{OMe})_2]$ dimer that bind to the vertices of the square-prism by the four μ_3 -hydroxides. The topology, and the highly reduced $[\text{V}^{\text{IV}}_8\text{V}^{\text{III}}_2]$ state, of **6** is unique for a polyoxoalkoxovanadate. This chemistry also highlights the importance of exploring a wide temperature range in cluster chemistry – under the higher temperature, solvothermal conditions this reaction gives a less oxidized, higher nuclearity product.

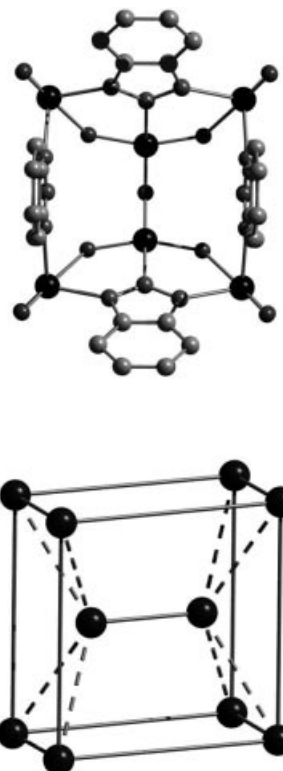


Figure 6. The molecular structure of complex **6** (top); and the $\{\text{V}^{\text{IV}}_8\}$ box encapsulating the $\{\text{V}^{\text{III}}_2\}$ fragment (bottom). Some of the MeO^- ions have been removed for clarity.

The magnetic properties of **6** are dominated by strong antiferromagnetic interactions: the room temperature $\chi_M T$ value of $3.3 \text{ cm}^3 \cdot \text{K} \cdot \text{mol}^{-1}$, is well short of the value expected for eight uncoupled V^{4+} and two V^{3+} ions, and is already rapidly decreasing with decreasing temperature. The low temperature value tends towards zero indicating a diamagnetic ground state for the cage. This strong antiferromagnetic coupling is consistent with the structure – very strong coupling is expected for the face-sharing $(\text{VO})_2$ pairs on the short edges of the box.

The majority of Single-Molecule Magnets (SMMs) reported to date have been clusters containing Mn^{3+} ions.^[4,19] In each case the clusters have been made, at least initially, via the serendipitous assembly of Mn starting materials

with flexible organic bridging ligands such as carboxylates or alkoxides. Manganese clusters often display “unusually” large spin ground states with respect to other 3d transition metals, and large and negative magnetoanisotropies resulting from the presence of Jahn–Teller distorted Mn^{3+} ions. However this presents a synthetic problem: there are few *simple* readily available sources of Mn^{3+} . This has resulted in the use of two alternative techniques. The first is the use of the basic metal carboxylates of general formula, $[\text{M}_3\text{O}(\text{RCO}_2)_6\text{L}_3]^{0/+}$, which can contain either two or three Mn^{3+} ions, and the second is the oxidation of Mn^{2+} salts with permanganate, MnO_4^- .^[4] Both of these techniques have been successful, particularly the former. An alternative approach is to use MnF_3 . The main disadvantage of using metal fluorides is their relative insolubility and therefore the apparent need for more “complicated” synthetic procedures – indeed the majority of fluoride-containing clusters have been isolated at elevated temperatures.^[20] For MnF_3 this insolubility can be easily overcome by using either a “melt” reaction whereby the BtaH acts as the solvent ($\text{MPt} = 100^\circ\text{C}$) in which the MnF_3 dissolves as the reaction proceeds,^[21] or by the simple reflux of the reaction mixture in a particular solvent. For example the complex $[\text{Mn}^{\text{III}}_{26}\text{O}_{17}(\text{OH})_8(\text{OMe})_4\text{F}_{10}(\text{Bta})_{22}(\text{MeOH})_{14}(\text{H}_2\text{O})_2]$ (**7**, Figure 7) is made by simply mixing MnF_3 and BtaH in MeOH at ca. 60°C . The rather complicated $[\text{Mn}^{\text{III}}_{26}\text{O}_{17}(\text{OH})_8(\text{OMe})_4]^{32+}$ core of **7** can be described as a central distorted tetra-face-capped octahedron either side of which are attached vertex-sharing tetrahedra. The O^{2-} ions all bridge in their usual μ_3 -fashion, forming $\{\text{Mn}_3\text{O}\}^{7+}$ triangular units. The OH^- ions are of two types: four are μ_3 -bridging and are situated within the tetra-face-capped octahedron, while the remaining ions are μ_2 -bridging and are situated both in the tetra-face-capped octahedron and within the two vertex-sharing tetrahedra. The 22 deprotonated Bta[−] ligands are of two types: four use all three nitrogens to bond to three Mn^{3+} centers while the remaining 18 use only two nitrogen atoms to bond to two Mn^{3+} centers, the third nitrogen atom H bonds to adjacent MeOH, H_2O or OH^- ligands. The four MeO^- ions are all μ_2 -bridging, but rather unusually there are also two MeOH molecules which act as μ_2 -bridges, whilst the ten F^- ions are bonded terminally. Fitting the magnetization (M vs. H) data for complex **7** gives $S = 4$, $g = 2.0$ and $D = -0.90\text{ cm}^{-1}$. AC susceptibility measurements performed on **7** in the 1.8–4.00 K range show the presence of out-of-phase ac susceptibility signals, but no peaks. Low-temperature single-crystal studies performed on **7** on an array of micro-SQUIDS^[22] show the time and temperature-dependent hysteresis loops indicative of single-molecule magnetism behavior (Figure 8). Below 1.2 K, hysteresis loops are observed in magnetization vs. field studies whose coercivities increase with decreasing temperature, at a sweep rate of 0.14 T/s. The loops do not show the step-like features associated with quantum tunneling of magnetization (QTM), and appear typical for a cluster with a distribution of energy barriers. The steps may be present but broadened out, due to the inherent disorder associated with the crystal of **7**,^[21] re-

sulting in a distribution of Mn^{3+} environments. These observations have been reported for other large SMMs.^[23] Relaxation data at very low temperatures were determined from dc relaxation decay measurements (Figure 9). The relaxation of crystals of SMMs is often very complicated, leading to non-exponential relaxation laws, and the M/M_s -vs- t curves for **7** cannot be fitted by a simple-exponential, stretched-exponential or square-root law. In order to extract the temperature dependence of the mean relaxation time $\tau(T)$, it is necessary to use a single scaling function $[t/\tau(T)]$.^[24] This scaling analysis allows $\tau(T)$ to be determined without making any particular assumption about the relaxation law, and allows the mean relaxation time $\tau(T)$ to be extracted. Fitting of these data to the Arrhenius law (Figure 9) gives an effective mean barrier for the reversal of magnetization of approximately 15 K and a pre-exponential factor of $\tau_0 = 3 \cdot 10^{-9}$ s. Below ca. 0.2 K, the relaxation rates become temperature-independent, strongly suggesting the presence of QTM in the ground state. The experimentally derived U_{eff} value of 15 K is comparable to the theoretical value ($U = S^2|D| \approx 21$ K). Indeed, U is expected to be larger than U_{eff} as the reversal of magnetization has two components: thermally activated relaxation over the barrier and quantum tunneling of magnetization (QTM) through the barrier.

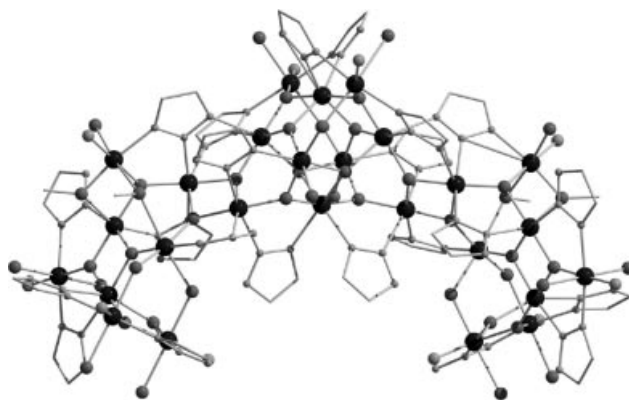


Figure 7. The molecular structure of complex **7**.

Repeating the reaction that produces complex **7** but in the presence of pyridine affords the decametallic complex $[\text{Mn}_{10}\text{O}_6(\text{OH})_2(\text{Bta})_8(\text{py})_8\text{F}_8]$ (**8**), while the same reaction in the presence of triethylamine produces the trimetallic species $[\text{NHEt}_3]_2[\text{Mn}_3\text{O}(\text{Bta})_6\text{F}_3]$ (**9**).^[21,25] Complex **8** (Figure 10) consists of a “supertetrahedral” $[\text{Mn}^{\text{III}}_{10}]$ core bridged by six $\mu_3\text{-O}^{2-}$ ions, two $\mu_3\text{-OH}^-$ ions, four $\mu_2\text{-F}^-$ ions and eight $\mu_2\text{-Bta}^-$ ions, while complex **9** (Figure 11) has a structure analogous to that of the basic metal carboxylates of general formula $[\text{M}_3\text{O}(\text{RCO}_2)_6\text{L}_3]^{0/+}$, consisting of an oxo-centered metal triangle with $\mu_2\text{-Bta}^-$ ligands bridging each edge of the triangle and the fluoride ions acting as the terminal “L” ligands. Both complexes display dominant antiferromagnetic exchange interactions resulting in small spin ground states. For complex **9**, the best fit to the experimental $\chi_M T$ vs. T data was obtained for the following pa-

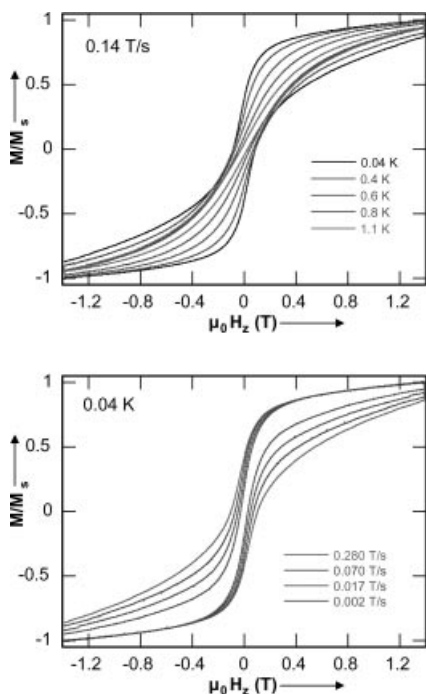


Figure 8. Magnetization (M) of **7** vs. applied magnetic field ($\mu_0 H$). The magnetization is normalized to its saturation value. The resulting hysteresis loops are shown at different temperatures and different field sweep.

rameters: $J_a = -5.01 \text{ cm}^{-1}$; $J_b = +9.16 \text{ cm}^{-1}$ and $g = 2.00$, resulting in an $S = 2$ spin ground state. DFT calculations, however, suggest an $S = 0$ ground state with $J_a = -2.95 \text{ cm}^{-1}$ and $J_b = -2.12 \text{ cm}^{-1}$ with two $S = 1$ states at 1.46 cm^{-1} and 5.9 cm^{-1} , and an $S = 2$ state at 6.1 cm^{-1} above the ground state.^[21] The presence of low-lying excited states leads to obvious problems when trying to satisfactorily fit the experimental data. The ground state of this molecule can be changed from $S = 0$ to $S = 2$ by small changes in the exchange interaction J_b . The ratio of J_a/J_b vs. the Eigen values obtained for these exchange parameters is shown in Figure 11. For a value of $J_a/J_b < 1$, the ground state spin value varies from $S = 2$ to $S = 1$; for $J_a/J_b = 1$ the ground state becomes $S = 0$, and for $J_a/J_b > 1$ the ground state varies from $S = 0$ to $S = 2$. For the DFT calculated values, the J_a/J_b ratio is found to be 1.37 and the ground state is $S = 0$. However, it is also clear that for $J_a/J_b > 1$ the energy levels are very closely separated, and the fact that the ground state depends on the ratio of J_a/J_b reveals that a degree of spin frustration exists in the triangle. At lower and higher values of J_a/J_b the degree of spin frustration is minimal, giving rise to an $S = 2$ ground state which can be accounted for by a simple pairwise exchange interaction. At intermediate values of J_a/J_b , spin frustration causes a net spin vector alignment, which cannot be accounted for by considering a simple pairwise exchange interaction, and the value of the ground state depends on the degree of spin frustration.^[21,25]

By replacing BtaH with its dimethyl derivative ($\text{Me}_2\text{-BtaH}$; 5,6-dimethylbenzotriazole) in otherwise similar reactions to those above affords completely different clusters: the octametallic complex $[\text{Mn}_8\text{O}_4(\text{OMe})_2(\text{Me}_2\text{Bta})_6\text{F}_8-$

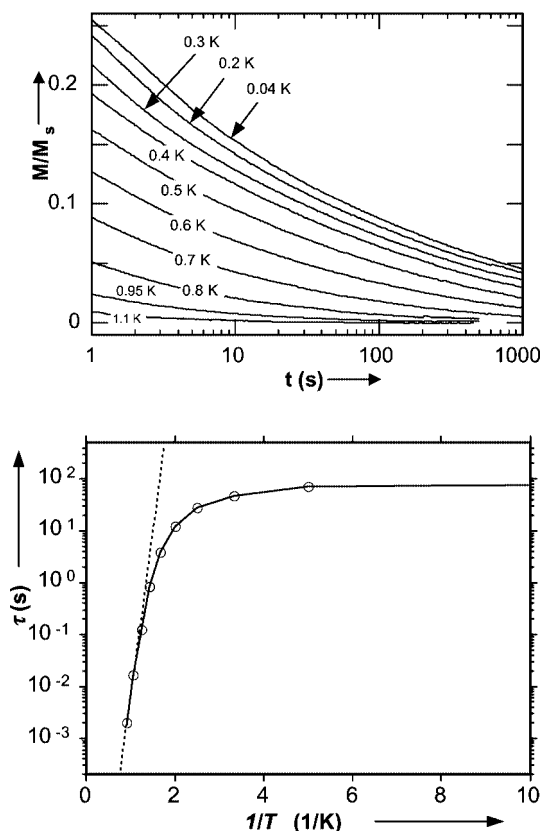


Figure 9. Relaxation data for **7** plotted as M/M_s vs. time, M is normalized to its saturation value (top); Arrhenius plot for **7** using dc decay data on a single crystal. The dashed line is the fit of the data in the thermally activated region.

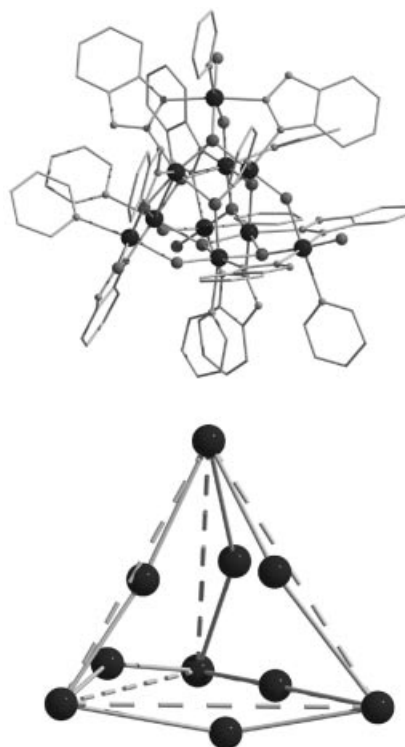


Figure 10. The molecular structure of complex **8** (top) and its supertetrahedral metallic core (bottom).

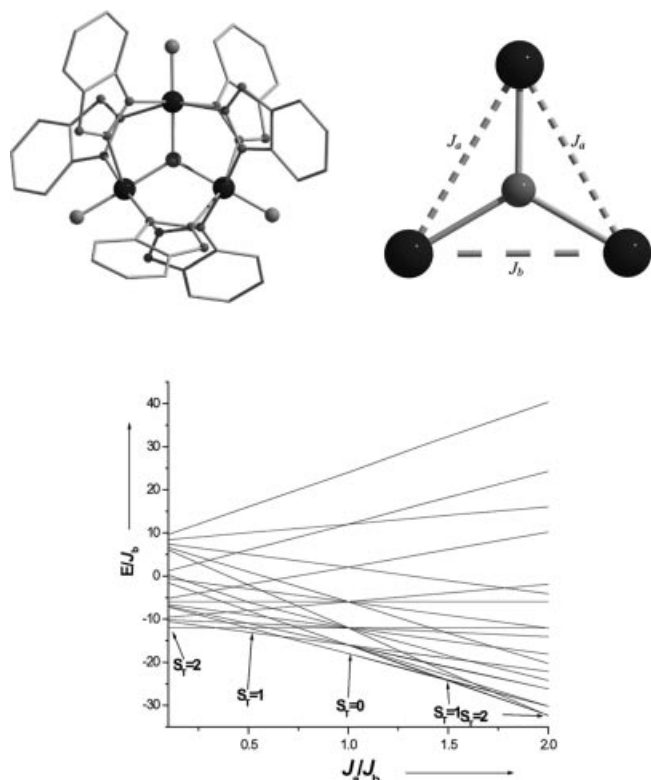


Figure 11. Top: Molecular structure of complex **9** and the two independent exchange interactions; bottom: Plot of calculated Eigen values vs. J_a/J_b for complex **9**. The experimental data was fitted with a two- J model that employed the spin Hamiltonian $\hat{H} = -2[J_a(\hat{S}_3\hat{S}_2) + J_a(\hat{S}_3\hat{S}_1) + J_b(\hat{S}_2\hat{S}_1)]$. For more details see ref.[21]

($\text{Me}_2\text{BtaH})(\text{MeOH})_8$ (**10**), and the tridecametallic complex $[\text{Mn}_{13}\text{O}_{12}(\text{Me}_2\text{Bta})_{12}\text{F}_6(\text{MeOH})_{10}(\text{H}_2\text{O})_2]$ (**11**).^[25] The core of **10** (Figure 12) consists of a central $[\text{Mn}_4\text{O}_2]^{8+}$ butterfly unit, the body atoms of which are also part of a peripheral $[\text{Mn}_3\text{O}]^{4+}$ triangular unit. The $[\text{Mn}_4\text{O}_2]$ butterfly is near planar with the two peripheral $[\text{Mn}_3\text{O}]$ triangles perpendicular to this plane, attached via an O^{2-} ion forming a $[\text{Mn}_8\text{O}_4]^{16+}$ core. Two MeO^- and two F^- ions act as μ_2 -bridges, the MeO^- bridging one side of the $[\text{Mn}_3\text{O}]$ unit and the F^- linking the $[\text{Mn}_3\text{O}]$ unit to the central $[\text{Mn}_4\text{O}_2]$ butterfly. The F^- bridges are asymmetric as, in each case, one Mn–F bond lies on a Jahn–Teller axis. The six Me_2Bta^- ligands all bond in a μ_2 -fashion and the remaining six F^- ions and eight MeOH molecules all are terminal. The core of **11** (Figure 13) consists of a $[\text{Mn}^{\text{IV}}_3\text{Mn}^{\text{III}}_4\text{O}_{12}]$ centered hexagon. The Mn^{4+} ions form a linear $[\text{Mn}_3\text{O}_4]$ trimer through the centre of the hexagon with the Mn^{3+} ions attached on either side. The twelve O^{2-} ions are all μ_3 -bridging and are of two types: six are bound to the central Mn^{4+} ion and link this ion to the outer six Mn ions of the hexagon. The remaining six O^{2-} ions bridge between the outer Mn ions of the centered-hexagon and the remaining six Mn^{3+} ions that are located, alternately, above and below the plane of the $[\text{Mn}^{\text{IV}}_3\text{Mn}^{\text{III}}_4\text{O}_{12}]$ core. The μ_2 - Me_2Bta^- ligands are all deprotonated and link the Mn ions in the central hexagon to the Mn ions above and below this plane.

The coordination of these six Mn ions is completed by a terminal F^- ion and either two MeOH molecules or one MeOH and one H_2O molecule. The central $[\text{Mn}^{\text{IV}}_3\text{Mn}^{\text{III}}_4\text{O}_{12}]$ core of **11** is reminiscent of the hexagonal close-packed structure present in CdI_2 and is similar to the cores found in several large cluster compounds.^[26] Magnetic studies reveal that both **10** and **11** have small spin ground states.

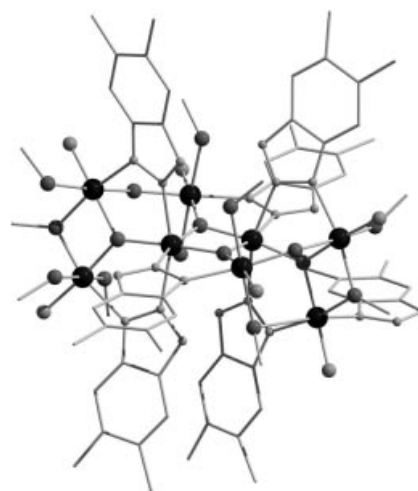


Figure 12. The molecular structure of complex **10**.

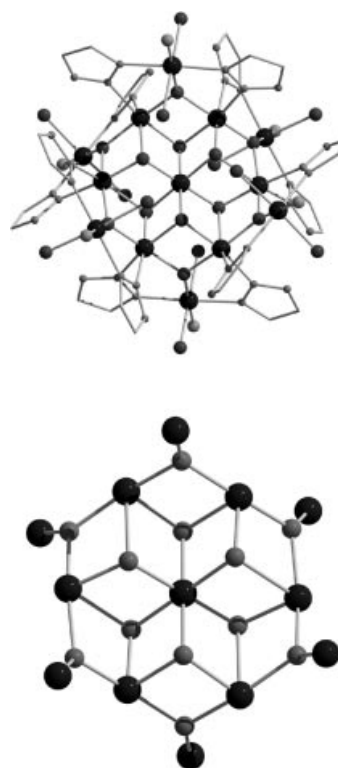


Figure 13. The molecular structure of complex **11** (top) and its metal-oxygen core (bottom).

Complexes **7–11** can all be described as aggregated $\{\text{Mn}_3\text{O}\}$ triangular units: compound **7** consists of twenty triangular units; **8** is made from eight edge-sharing units; **9** consists of one triangular unit; **10** contains four edge- and vertex-sharing units; and **11** contains twelve such units. This perhaps suggests that triangular $[\text{Mn}_3\text{OF}_3]^{4+}$ units may be present in all of the above solutions and that the identity of the isolated crystalline product is then dependent on the nature of the added base. Indeed complex **10** could be thought of as an “intermediate” in the formation of **11**: both clusters are comprised of aggregated $\{\text{Mn}_3\text{O}\}$ units and the $\{\text{Mn}_8\text{O}_4\}$ unit present in **10** can be seen three times in the core of **11**.

Conclusions

The work here clearly illustrates that the use of benzotriazole and its analogues is a successful synthetic strategy for the formation of large polymetallic cluster compounds. The complexes isolated thus far range in nuclearity from three to twenty six and in topologies (amongst others) ranging from simple triangles and tetrahedra, to rectangular boxes, supertetrahedra and hexacapped hexagonal prisms. Some of these complexes have displayed interesting magnetic properties including some of the largest spin ground states ever seen and single-molecule magnetism behavior. The science remains in its infancy, but given our initial results the future promises many more exciting complexes.

Acknowledgments

We would like to thank the EPSRC, Leverhulme Trust and Lloyd's of London Tercentenary Foundation for financial assistance (UK). The EC (HPRN-CT-1999-00012)/TMR network “Molnanomag”, and MRTN-CT-2003-504880 “QuEMolNa”. The work described has been done in collaboration with a number of groups. In particular, the authors would like to thank Prof George Christou (University of Florida), Dr Wolfgang Wernsdorfer (Laboratoire Louis Néel), Prof Talal Mallah (Université Paris-Sud), Drs Marco Evangelisti and Marco Affronte (INFM-CNR, Modena), Drs Guillem Aromí and Joan Cano (Universitat de Barcelona). EKB, EJLM and DC would also like to thank Drs Leigh Jones, David Low, Rebecca Laye and Gopalan Rajaraman for their invaluable contribution to this work.

- [1] a) R. Sessoli, H.-L. Tsai, A. R. Schake, S. Wang, J. B. Vincent, K. Folting, D. Gatteschi, G. Christou, D. N. Hendrickson, *J. Am. Chem. Soc.* **1993**, *115*, 1804; b) R. Sessoli, D. Gatteschi, A. Caneschi, M. A. Novak, *Nature* **1993**, *365*, 141; c) R. Sessoli, D. Gatteschi, D. N. Hendrickson, G. Christou, *MRS Bull.* **2000**, *25*, 66.
- [2] See for example a) D. N. Hendrickson, G. Christou, H. Ishimoto, J. Yoo, E. K. Brechin, A. Yamaguchi, E. M. Rumberger, S. M. J. Aubin, Z. Sun, G. Aromí, *Mol. Cryst. Liq. Cryst.* **2002**, *376*, 301; E. K. Brechin, *Chem. Commun.* **2005**, 5141.
- [3] a) M. N. Leuenberger, D. Loss, *Nature* **2001**, *410*, 789; b) W. Wernsdorfer, N. Aliaga-Acalde, D. N. Hendrickson, G. Christou, *Nature* **2002**, *416*, 406; c) S. Hill, R. S. Edwards, N. Aliaga-Acalde, G. Christou, *Science* **2003**, *302*, 1015; d) J. Tejada, E. M. Chudnovsky, E. del Barco, J. M. Hernandez, T. P. Spiller, *Nanotechnology* **2001**, *12*, 181; e) E. J. L. McInnes, *Struct. Bond.* **2006**, *122*, in press.
- [4] E. K. Brechin, G. Aromí, *Struct. Bond.*, DOI: 10.1007/430_022.
- [5] I. Dugdale, J. B. Cotton, *Corros. Sci.* **1963**, *3*, 69.
- [6] a) M. Murrie, D. Collison, C. D. Garner, M. Helliwell, P. A. Tasker, S. S. Turner, *Polyhedron* **1998**, *17*, 3031; b) J. H. Marshall, *Inorg. Chem.* **1978**, *17*, 3711; c) J. Handley, D. Collison, C. D. Garner, M. Helliwell, R. Docherty, J. R. Lawson, P. A. Tasker, *Angew. Chem. Int. Ed. Engl.* **1993**, *32*, 1036; d) E. G. Bakalbassis, E. Diamantopoulou, S. P. Perlepes, C. P. Raptopoulou, V. Tangoulis, A. Terzis, T. F. Zafiropoulos, *J. Chem. Soc., Chem. Commun.* **1995**, 1347; e) V. Tangoulis, C. P. Raptopoulou, A. Terzis, E. G. Bakalbassis, E. Diamantopoulou, S. P. Perlepes, *Inorg. Chem.* **1998**, *37*, 3142.
- [7] V. Tangoulis, C. P. Raptopoulou, A. Terzis, E. G. Bakalbassis, E. Diamantopoulou, S. P. Perlepes, *Mol. Cryst. Liq. Cryst.* **1999**, *335*, 463.
- [8] I. Sotofte, K. Nielsen, *Acta Chem. Scand.* **1984**, *38*, 253.
- [9] A. L. Spek, A. R. Siedle, J. Reedijk, *Inorg. Chim. Acta* **1985**, *100*, L15.
- [10] B. Machura, J. O. Dziegielewski, R. Kruszynski, T. J. Batczak, *Polyhedron* **2003**, *22*, 2869.
- [11] I. Ino, J. C. Zhong, M. Munakata, T. Kuroda-Sowa, M. Maekawa, Y. Suenaga, Y. Kitamori, *Inorg. Chem.* **2000**, *39*, 4273.
- [12] J. Tabernor, L. F. Jones, S. L. Heath, C. Muryn, G. Aromí, J. Ribas, E. K. Brechin, D. Collison, *Dalton Trans.* **2004**, 975.
- [13] D. M. Low, L. F. Jones, A. Bell, E. K. Brechin, T. Mallah, E. Rivière, S. J. Teat, E. J. L. McInnes, J. L. Eric, *Angew. Chem. Int. Ed.* **2003**, *42*, 3781.
- [14] G. Rajaraman, J. Cano, E. K. Brechin, E. J. L. McInnes, *Chem. Commun.* **2004**, 1476.
- [15] M. Evangelisti, A. Candini, A. Ghirri, M. Affronte, E. K. Brechin, E. J. L. McInnes, *Appl. Phys. Lett.* **2005**, *87*, 072504.
- [16] A. L. Lima, K. A. Gschneider Jr, V. K. Pecharsky, A. O. Pecharsky, *Phys. Rev. B* **2003**, *68*, 134409.
- [17] D. M. Low, L. F. Jones, R. Laye, T. Mallah, E. Rivière, S. J. Teat, E. K. Brechin, E. J. L. McInnes, manuscript in preparation.
- [18] R. H. Laye, Q. Wei, P. Mason, E. Shanmugan, E. K. Brechin, E. J. L. McInnes, *J. Am. Chem. Soc.* **2006**, submitted.
- [19] G. Christou, *Polyhedron* **2005**, *24*, 2065.
- [20] a) E. J. L. McInnes, S. Piligkos, G. A. Timco, R. E. P. Winpenny, *Coord. Chem. Rev.* **2005**, *249*, 2577; b) N. V. Gerbeleu, Y. T. Struchkov, G. A. Timco, A. S. Batsanov, K. M. Indrichan, G. A. Popovic, *Dokl. Chem.* **1991**, *313*, 232; c) N. V. Gerbeleu, Y. T. Struchkov, G. A. Timco, A. S. Batsanov, K. M. Indrichan, G. A. Popovic, *Dokl. Akad. Nauk SSSR* **1991**, *313*, 1459; d) F. K. Larsen, J. Overgaard, S. Parsons, E. Rentschler, A. A. Smith, G. A. Timco, R. E. P. Winpenny, *Angew. Chem. Int. Ed.* **2003**, *42*, 5978; e) A. Bino, M. Ardon, D. Lee, B. Spingler, S. J. Lippard, *J. Am. Chem. Soc.* **2002**, *124*, 4578; f) E. M. Rumberger, L. N. Zakharov, A. L. Rheingold, D. N. Hendrickson, *Inorg. Chem.* **2004**, *43*, 6531.
- [21] L. F. Jones, G. Rajaraman, J. Brockman, M. Murugesu, J. Raftery, S. J. Teat, W. Wernsdorfer, G. Christou, E. K. Brechin, D. Collison, *Chem. Eur. J.* **2004**, *10*, 5180.
- [22] W. Wernsdorfer, *Adv. Chem. Phys.* **2001**, *118*, 99.
- [23] a) M. Soler, W. Wernsdorfer, K. Folting, M. Pink, G. Christou, *J. Am. Chem. Soc.* **2004**, *126*, 2156; b) A. J. Tasiopolous, A. Vinslava, W. Wernsdorfer, K. A. Abboud, G. Christou, *Angew. Chem. Int. Ed.* **2004**, *43*, 2117.
- [24] L. Thomas, A. Caneschi, B. Barbara, *Phys. Rev. Lett.* **1999**, *83*, 2398.
- [25] a) L. F. Jones, E. K. Brechin, D. Collison, J. Raftery, S. J. Teat, *Inorg. Chem.* **2003**, *42*, 6971; b) L. F. Jones, J. Raftery, S. J. Teat, D. Collison, E. K. Brechin, *Polyhedron* **2005**, *24*, 2443.

[26] See for example a) E. K. Brechin, S. G. Harris, A. Harrison, S. Parsons, A. G. Whittaker, R. E. P. Winpenny, *Chem. Commun.* **1997**, 653; b) A. K. Powell, S. L. Heath, D. Gatteschi, L. Pardi, R. Sessoli, G. Spina, F. Del Giallo, F. Pieralli, *J. Am. Chem. Soc.* **1995**, *117*, 2491; c) D. J. Price, S. R. Batten, B. Moubaraki,

K. S. Murray, *Chem. Commun.* **2002**, 762; d) J. T. Brockman, J. C. Huffman, G. Christou, *Angew. Chem. Int. Ed.* **2002**, *41*, 2506.

Received: March 8, 2006

Published Online: June 1, 2006